Available online at www.sciencedirect.com

SciVerse ScienceDirect

Ceramics International 38 (2012) 3713–3722

CERAMICS INTERNATIONAL

www.elsevier.com/locate/ceramint

Processing of graded anode-supported micro-tubular SOFCs based on samaria-doped ceria via gel-casting and spray-coating

M. Morales [a,*], M.E. Navarro [a], X.G. Capdevila [a], J.J. Roa [b], M. Segarra [a]

[a] Centre DIOPMA, Departament de Ciència dels Materials i Enginyeria Metal·lúrgica, Universitat de Barcelona, C/Martí i Franqués 1, 08028 Barcelona, Spain
[b] Institute Pprime, Laboratoire de Physique et Mécanique des Matériaux, CNRS-Université de Poitiers-ENSMA, UPR 3346, Bd Pierre et Marie Curie, BP 30179, 86962 Futuroscope Chasseneuil Cedex, France

Received 16 October 2011; received in revised form 18 December 2011; accepted 6 January 2012
Available online 15 January 2012

Abstract

A simple gel-casting method was successfully combined with the spray-coating technique to manufacture graded anode-supported micro-tubular solid oxide fuel cells (MT-SOFCs) based on samaria-doped ceria (SDC) as an electrolyte. Micro-tubular anodes were shaped by a gel-casting method based on a new and simple forming technique that operates as a syringe. The aqueous slurry formulation of the NiO–SDC substrate using agarose as a gelling agent, and the effect of spray-coating parameters used to deposit the anode functional layers (AFLs) and electrolyte were investigated. Furthermore, pre-sintering temperature of anode substrates was systematically studied to avoid the anode–electrolyte delamination and obtain a dense electrolyte without cracks, after co-sintering process at 1450 °C. Despite the high shrinkage of substrate (~70%), an anode porosity of ~37% was achieved. MT-SOFCs with ~2.5 mm of outer diameter, 370 μm thick substrate, 20 μm thick AFLs and 15 μm thick electrolyte were successfully obtained. The use of AFLs with 30:70 and 50:50 wt% NiO–SDC allowed to obtain a continuous gradation of composition and porosity in the anode–electrolyte interface.

Keywords: SOFC; Micro-tubular SOFC; Graded anode; Doped ceria; Gel-casting; Spray-coating

1. Introduction

Last decade, a great interest in the development of SOFCs for portable devices has been generated [1–4]. In order to achieve this goal, new configuration designs, materials and processing methods have been developed [5]. Among alternatives, micro-tubular SOFCs (MT-SOFCs) present several advantages in comparison with planar configuration: a rapid start-up and shut-down operation [6], high long term structural stability, high thermal-shock resistance [7], and high volumetric output power density [8,9]. In addition, the research in the field of micro-tubular SOFCs has followed the same patterns pursued to reduce the operating temperature in large-scale and planar SOFCs [10–12]. For this purpose, there are two main strategies: to decrease the electrolyte thickness in order to reduce its ohmic resistance losses, using anode-supported thin-film electrolytes in micro-tubular configuration [13,14]; and/or to use an electrolyte material with high ionic conductivity at intermediate temperatures (500–700 °C), such as gadolinium (GDC) or samarium doped ceria (SDC) [15–17].

In terms of manufacturing, the most common technique for MT-SOFCs processing is the traditional extrusion method, but it presents several difficulties such as a relatively high investment in equipment, and long time for the adjustment of processing parameters [18,19]. Aqueous gel-casting is a well-known colloidal processing method that presents several advantages with respect to conventional shaping processes, for instance extrusion or isostatic pressing [13,19,20]. First of all, it can be used to prepare ceramic modules from dense to porous with high quality and complex shaped [21]. Secondly, green body has enough strength being handled without shaping distortion [22]. Moreover, gel-casting processing exhibits a short forming time, high yields and low-cost equipment [23]. So, it can be used to shape the tubular fuel cell both in laboratory and at industry scale [24,25]. In the early gel-casting developed systems, acrylic monomers were used as gelling agents in organic solvents [26]. Owing to the toxicity of these

* Corresponding author.
E-mail addresses: mmorales@ub.edu, mmoralescomas@yahoo.es (M. Morales).

0272-8842/$36.00
doi:10.1016/j.ceramint.2012.01.015

systems, various alternatives based on aqueous monomers have been proposed [27]. Natural polysaccharides, such as agar and agarose, have been used as gelling agents, which form a gel on cooling, thus exhibiting large similarities to the principles of injection moulding [23].

On the other hand, another effective way to enhance the cell performance and prevent the quick cell degradation can be the use of an anode functional layer (AFL) between the anode substrate and electrolyte. The AFL should have a gradient in particle size and Ni content, thus obtaining a gradient of porosity, electrical conductivity and thermal expansion coefficient (TEC) [28]. It can be achieved by using a compositional graded functional layer with several sub-layers [29]. According to different previous works [28,30,31], an AFL thickness of 10–40 μm seems to be appropriately selected to enhance the cell performance. Among the deposition methods of composite layers [32,33], spray-coating technique is one approach for low-cost production with high potential to control the quality and thickness of cell layers [34]. In the simplest way, this method is performed with no handling, thus presenting a highly reproducible process. However, some efforts on timing and nozzle stabilization optimization are needed to acquire control over consistent deposition thickness with good results. A normal setup requires the adjustment of several spray parameters such as the spray nozzle to be placed over a substrate, and the rotational speed of substrate.

Up to date, most of the MT-SOFC works have been focused on the manufacture of anode-supported cells using yttria-stabilized zirconia (YSZ) as an electrolyte. However, only some researchers have processed small-scale tubular SOFCs based on doped ceria [13,35]. Most of these MT-SOFCs were shaped by isostatic pressing or traditional extrusion methods [13,18]. In this work, we present the processing of anode-supported MT-SOFCs with a SDC electrolyte using the gel-casting and spray-coating techniques. Although it has been reported by some researchers, the effect of multiple processing parameters on the substrate and coating characteristics has rarely been reported in detail. Therefore, the purpose of this study was to investigate the influence of the gel-casting and spray-coating parameters on the characteristics of both substrate and coatings for MT-SOFCs based on SDC electrolyte. First, a useful formulation based on aqueous suspension of agarose for gel-casting was obtained. Afterwards, micro-tubular anodes were shaped by gel-casting method based on a new, simple and low-cost forming technique, which operates as a syringe. Secondly, thin-films of NiO–SDC as a graded AFL, SDC as an electrolyte and cobaltite–SDC as a cathode were deposited by spray-coating method. A suitable spray setting was determined to control the thickness and quality of every layer. Before electrolyte deposition, anode substrates with AFLs were pre-sintered to avoid the delamination of the anode–electrolyte interface, and obtain a dense electrolyte without cracks after co-sintering process. Thus, the effect of pre-sintering temperature on anode support shrinkage was systematically studied. The microstructures of the different components of the MT-SOFCs were evaluated by scanning electron microscopy (SEM).

2. Experimental procedure

2.1. Synthesis and characterization of the materials

Samarium-doped ceria, nickel oxide-samarium doped ceria (60:40, 50:50, and 30:70 wt%), and lanthanum strontium cobaltite powders, with a nominal composition of $Sm_{0.2}Ce_{0.8}O_{1.9}$, NiO–$Sm_{0.2}Ce_{0.8}O_{1.9}$ (NiO–SDC) and $La_{0.6}Sr_{0.4}CoO_3$ (LSC), respectively, were synthesized by polyacrylamide gel combustion as described elsewhere [36–38]. The materials were prepared from Sm_2O_3 (Strem Chemical 99.9%), CeO_2 (Strem Chemical 99.9%), La_2O_3 (Alfa Aesar 99.9%), $Sr(CH_3COO)_2$ (Pro-BVS 99%), $Ni(CH_3COO)_2$ (Alfa Aesar 99%) and $Co(CH_3COO)_2$ (PANREAC 99%). After combustion, the materials were calcined at 500 °C for 2 h to assure the total organic removal [36], and further milled. All these powders were characterized by BET specific surface and XRD.

2.2. Preparation and characterization of the suspensions

Porous anode tubes were prepared by aqueous gel-casting method. Ceramic suspensions with anode powder and distilled water were prepared by adding a commercial dispersant (DOLAPIX Zschimmer & Schwarz España, S.A.). Suspension homogenization was performed by an ultrasonic finger (Sonics Vibracell VCX-130). Agarose solution was prepared by adding an industrial agar (Conda Lab.) and then activated by heating above 80 °C. The agarose solution was maintained above 60 °C until casting in order to avoid a premature gelation. Furthermore, the suspension viscosity was determined within temperature range of 40–60 °C using a viscosimeter (HAAKE Viscotester 6R plus). In this step, the optimization of several process parameters such as solid loading (22–30 wt%), dispersant concentration (0.5–2.0 wt%) and agarose amount (0.5–2 wt%) was investigated.

2.3. Cell manufacturing

The experimental procedure to prepare the MT-SOFCs is shown in Fig. 1. First of all, the NiO–SDC tubes were extruded from the gel-casting using a steel punch (Ø 3 mm) with an in-house-designed aluminium die (Ø 6 mm and length = 20 cm), which is exhibited in Fig. 2. It presents two different sections: the reservoir and the syringe. The reservoir, which contains the slurry, is closed and made of silicone to avoid temperature gradients and a premature gelation of slurry; it is also conical to allow a free flow of the slurry towards the syringe. The plunger can be moved by hand, pulling or pushing along the tube, thus allowing to take in, gelify and expel the body through the open end of the tube. The resulting green tubes were dried in air for 24 h. They were then cut to a length of 6 cm. After finishing the process, the total (open and closed) porosity of anode substrate was determined from the difference between the theoretical and real densities, and using a helium gas absorption pycnometer (Micromeritics) to determine the apparent density.

After shaping the tubular anodes, two anode functional layers (AFL I and II) with the compositions of 30:70 and

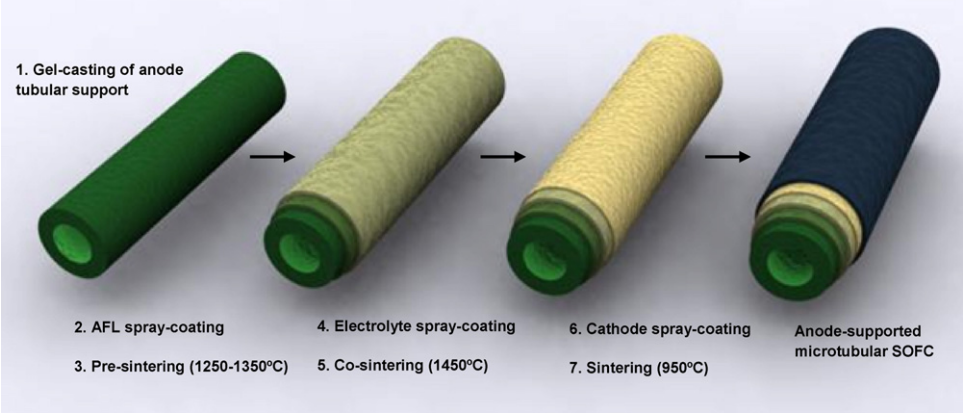

Fig. 1. Schematic diagram of the manufacturing of the anode-supported micro-tubular SOFC.

50:50 wt% NiO–SDC and within the thickness range of 10–20 μm were deposited by spray-coating onto the tubular substrates. The inks, which consisted of NiO–SDC as the solid loading and terpineol as the solvent (1:5 wt%), were prepared to have low viscosity, high volatility, and moderate particle loading. These properties were chosen to achieve a suitable atomization and a quick drying of the ceramic inks at room temperature. The final suspensions were ultrasonically mixed. An air pressure-assisted spray was used to deposit the NiO–SDC colloidal slurry onto the rotating tubular substrate to obtain the different thin-films. The spraying conditions, such as the air pressure of nozzle to control both air and ink flow rates, the rotational speed of tubular substrate, the nozzle speed, and the distance between the nozzle and the substrate, were set up to deposit each anode functional layer within a low number of spray cycles. The anode layers of the tubular half-cell were then dried in air and further were pre-sintered in air at different temperatures between 1250 and 1350 °C for 1 h.

Afterwards, a SDC electrolyte layer was coated onto the surface of each pre-sintered tube using the spray-coating method. Previously to the colloidal spraying deposition of the SDC powders, a detailed study of the attrition milling conditions was carried out to remove the formation of large agglomerates of the nanopowders synthesized, and to decrease their particle size in order to improve their sintering properties and densification behaviour. So, they were ball-milled in ethanol media for more than 6 h at 300 rpm using a zirconia jar and yttria balls (5 mm in diameter). As the different colloidal suspensions of NiO–SDC, the SDC colloidal suspension for spray-coating was also prepared by mixing the SDC powder with terpineol (1:5 wt%) and ultrasonically mixed. The SDC colloidal suspension was then spray-coated on the different anodes to obtain a film thickness around 15 μm. The film electrolyte of the tubular half-cell was dried in air. Then, both anode and electrolyte were co-sintered at a temperature of 1450 °C for 5 h in order to obtain a porous anode and a dense electrolyte, without using sintering additives that allow to decrease the densification temperature of SDC.

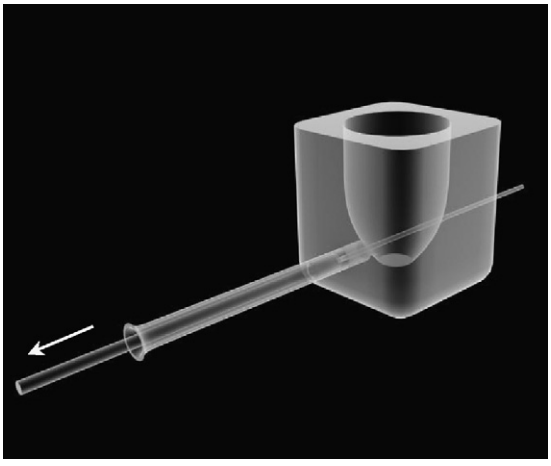

Fig. 2. Schematic illustration of the system to shape tubular anodes.

Finally, the anode tubes with electrolyte were spray-coated with a cathode suspension. Cathode powders were firstly milled for 60 s in a ring mill. The 70:30 wt% LSC–SDC precursor was also mixed with terpineol (1:5 wt%) to make the colloidal suspension, and sprayed onto the SDC electrolyte of NiO–SDC/SDC tube. The conditions of cathode spray-coating were similar to those of the AFLs and electrolyte. As described elsewhere [11], the tubes were sintered at a temperature of 950 °C in air for 5 h to complete the cell. The fuel cell microstructure was examined by scanning electron microscopy (SEM Hitachi H-2300).

3. Results and discussion

3.1. Properties of powders

The XRD patterns of NiO–SDC, SDC and LSC powders presented no evidences of secondary phases (Fig. 3). After ring-milling for 60 s, NiO–SDC powders with different compositions (60:40, 50:50, and 30:70 wt%) were analysed by BET technique, thus obtaining a specific surface of 30–40 m^2/g and a mean particle size of 20–30 nm. On the other hand, the microstructure of the SDC coating strongly depends on the degree of the powder agglomeration between particles in the colloidal suspension. A suitable and fast sintering kinetics of this material can be achieved with a low powder agglomeration, thus obtaining a high coating density. After

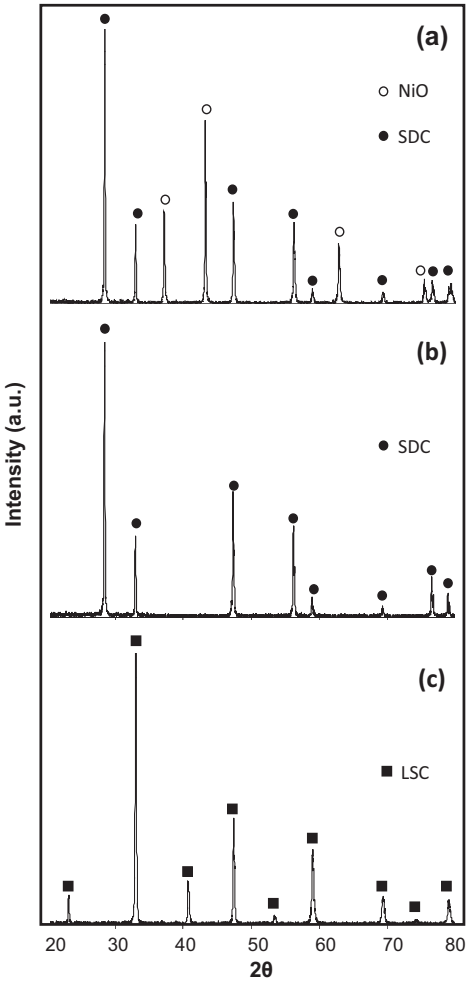

Fig. 3. X-ray diffraction patterns for: (a) NiO–SDC (60:40 wt%); (b) SDC; and (c) LSC as synthesized.

ball-milling for 6 h, the presence of the big agglomerates (>100 μm), which were generated during the combustion and calcination processes, was strongly decreased leading to a maximum particle size. Finally, the properties of LSC powders were determined, after ring-milling for 60 s, thus obtaining a specific surface of 45 m^2/g and a mean particle size of 80 nm.

3.2. Formulation of suspension for gel-casting process

Our preliminary experiments indicated that the study ranges for the different process parameters were: solid loading amount of 22–30 wt% vs. distilled water, dispersant concentration of 0.5–2 wt% vs. powder, and agarose content of 0.5–2 wt% vs. solid loading. According to a previous work [39], the concentrations of the solid loading and/or agarose in the suspensions, which are suitable for casting, were determined by the suspension viscosity and the strength of the cast green body. So, it was necessary to adjust the agarose and NiO–SDC contents in order to achieve a suitable workability of the paste. Moreover, a higher solid loading in the suspension led to a higher suspension viscosity and also a higher density of the final ceramic. However, the SOFC anodes should be porous, and therefore, a low solid loading is required. Furthermore, the gelation of the ceramic suspensions was initiated around 40 °C, depending on the agarose concentration. In order to avoid a premature gelation, before casting, these mixtures were maintained above 60 °C. So, it was interesting to determine the viscosity within the temperature range of 40–60 °C.

Table 1 shows the properties of different formulations of suspensions for the gel-casting system. In order to disperse anode powder in distilled water, it was necessary to add the 1 wt% vs. powder of a commercial dispersant. When the dispersant concentration was higher than 1.5 wt%, the NiO–SDC was coarsened again. For low concentrations of agarose, the bodies deformed due to the low strength of the cast green bodies during drying process. When the solid loading and/or the agarose content was too high, the high viscosity was not suitable for casting, thus becoming difficult to fill the mould. It was found that for 22–30 wt% powder/water and around 1 wt% vs. water is the minimum agarose amount to obtain a green tube with suitable mechanical properties, thus avoiding its plastic deformation during handling. Among the slurry formulations 4, 5 and 6, the last one was chosen for casting. In comparison with the other formulations, it allows to achieve the maximum solid

Table 1
Properties of the different formulations of suspensions for 1 wt% commercial dispersant vs. solid loading.

Formulation no.	Solid loading (wt% vs. distilled water)	Agarose (wt% vs. solid loading)	Viscosity at 60–40 °C (mPa s)	Paste for casting	Observations
1	22	0.75	∼200 to 1500	Workable	Plastically deformed during handling and/or by its own weight
2	26				
3	30				
4	22	1.00	∼500 to 2000	Workable	Suitable strength
5	26				
6	30				
7	22	1.25	∼1500 to 3000	Workable	Cracked surface during drying
8	26				
9	30				
10	22	1.50	>2500	Unworkable	Cracked body during drying
11	26				
12	30				

loading, thus minimizing the shrinkage during drying and sintering processes.

Finally, the tubes were shaped using formulation 6, as described in the previous section. After drying in air for 24 h, the gel-casting anode supported tubes were round and straight. The dimensions of the dried tubes were: ∼5 mm of outer diameter and ∼18 cm of length. Finally, they were cut to a length of 6 cm.

3.3. Colloidal spray deposition of AFLs and electrolyte

The thickness and quality of each layer depends on different spray-coating variables. Effective settings for each variable were determined, thus allowing to adjust the layer thickness with a low number of spray cycles. A nozzle speed of 20 cm min^{-1} was used, because it is constant in our system. The highest rotational speed of tubular substrate was selected to improve the layer homogeneity and the removal of the organic phase, thus increasing the drying rate during deposition. The shortest possible distance from spray nozzle to substrate was chosen. In order to avoid a insufficient organic solvent quantity and the presence of ink splashes at impact onto the substrate, thus achieving a good substrate wet out. Finally, the air pressure of nozzle to control both air and ink flow rates was selected to combine a suitable atomization and drying rate of layer. Therefore, for the prepared inks and a nozzle speed of 20 cm min^{-1}, a rotational speed of 200 rpm, nozzle-to-substrate distance of 15 mm and air pressure of 0.7 bar were suitable conditions to deposit both NiO–SDC colloidal suspensions onto the rotating tubular substrates. As shown in Fig. 4, the thickness of the AFLs increased almost linearly with the spray-coating cycles within the range of 1–6 times. So, 2 and 3 cycles of spray-coating were necessary to adjust the AFLs thickness to 10 and 20 μm, which seems to be appropriately selected to enhance the cell performance according to several previous works [28,30,31]. Afterwards, the samples were pre-sintered in air at an optimal temperature within the range of 1250–1350 °C for 1 h, which will be studied in the next section.

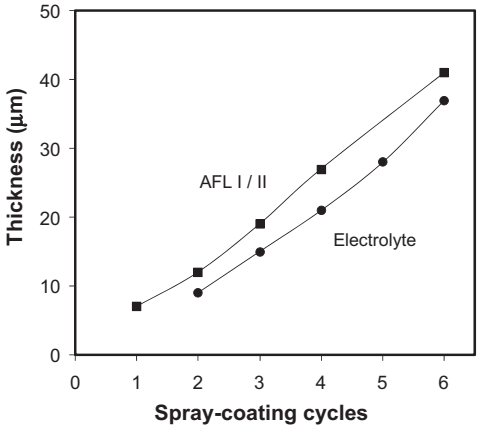

Fig. 4. Thickness of the electrolyte, AFL I and II layers as a function of spray-coating cycles.

The next operation of the MT-SOFC fabrication required the electrolyte deposition by spray-coating. Using the same effective spray-coating settings to deposit the AFLs, the thickness of the SDC electrolyte also increased linearly with the number of spray-coating cycles (Fig. 4). In order to deposit a determined layer thickness of electrolyte, it was necessary one more spray-coating cycle more than those for AFLs. It was attributed to the porosity difference between the AFLs and the electrolyte. Three cycles of spray-coating were performed to adjust the SDC layer thickness to ∼15 μm, which allows to obtain a good cell performance according to several previous works [13,31]. Subsequently, the electrolyte, AFLs and anode substrate were co-sintered at 1450 °C for 5 h in air. The co-sintering temperature was selected to achieve a dense SDC film, without using sintering additives that allow to decrease the densification temperature of SDC.

SEM images of anode–electrolyte interfaces for two half-cells with total AFL thicknesses (that is AFL I and II) of 20 μm (Fig. 5a and b) and of 40 μm (Fig. 5c and d) are shown. So, the thicknesses of anode functional layers were close to that of an electrolyte. The SDC layers of both half-cells were dense, and free of cracks and pinholes, except for some isolated pores. However, no cross-layer pores or cracks were observed. The interfaces of both half-cells presented a continuous gradation of the porosity (Fig. 5a and c) and the composition of NiO and SDC (Fig. 5b and d). The bright grey phase is SDC and the dispersed grains are NiO. Thus SDC phase forms well-distributed ceramic skeleton and nickel grains connected with each other. Good adhesions between substrate–AFL I, AFL I–AFL II and AFL II–electrolyte were achieved. While the interface of AFL I and II can be clearly observed, the one of AFL II and anode substrate is difficult to distinguish, because of their close compositions and a good integration. So, the microstructure of anode substrate is more porous than that of AFLs.

3.4. Effect of pre-sintering temperature

Generally, the sintering shrinkage of the anode-support should be equal to or slightly higher than that of the electrolyte layer to obtain a uniform, continuous, and dense one, and avoid the delamination of the anode–electrolyte interface. In addition, it improves the densification of the electrolyte film, due to the compression stresses induced on it. In the present work, the shrinkages of anode-support and electrolyte during co-sintering at 1450 °C for 5 h were determined in preliminary experiments. The shrinkage measurements were performed on a NiO–SDC tubular support obtained by gel-casting process and a compact pellet of SDC powder made by uniaxial pressing method (200 MPa), and not on deposited layers. Therefore, these values were roughly approximate. Tubular anodes and SDC pellets exhibited sintering shrinkages of ∼70 and ∼30%, respectively. Owing to the large shrinkage difference between both materials, it was necessary a pre-sintering process of the tubular substrates with AFLs to decrease their shrinkage during co-sintering with electrolyte process. They were pre-sintered in air at different temperatures between 1250 and 1350 °C for 1 h.

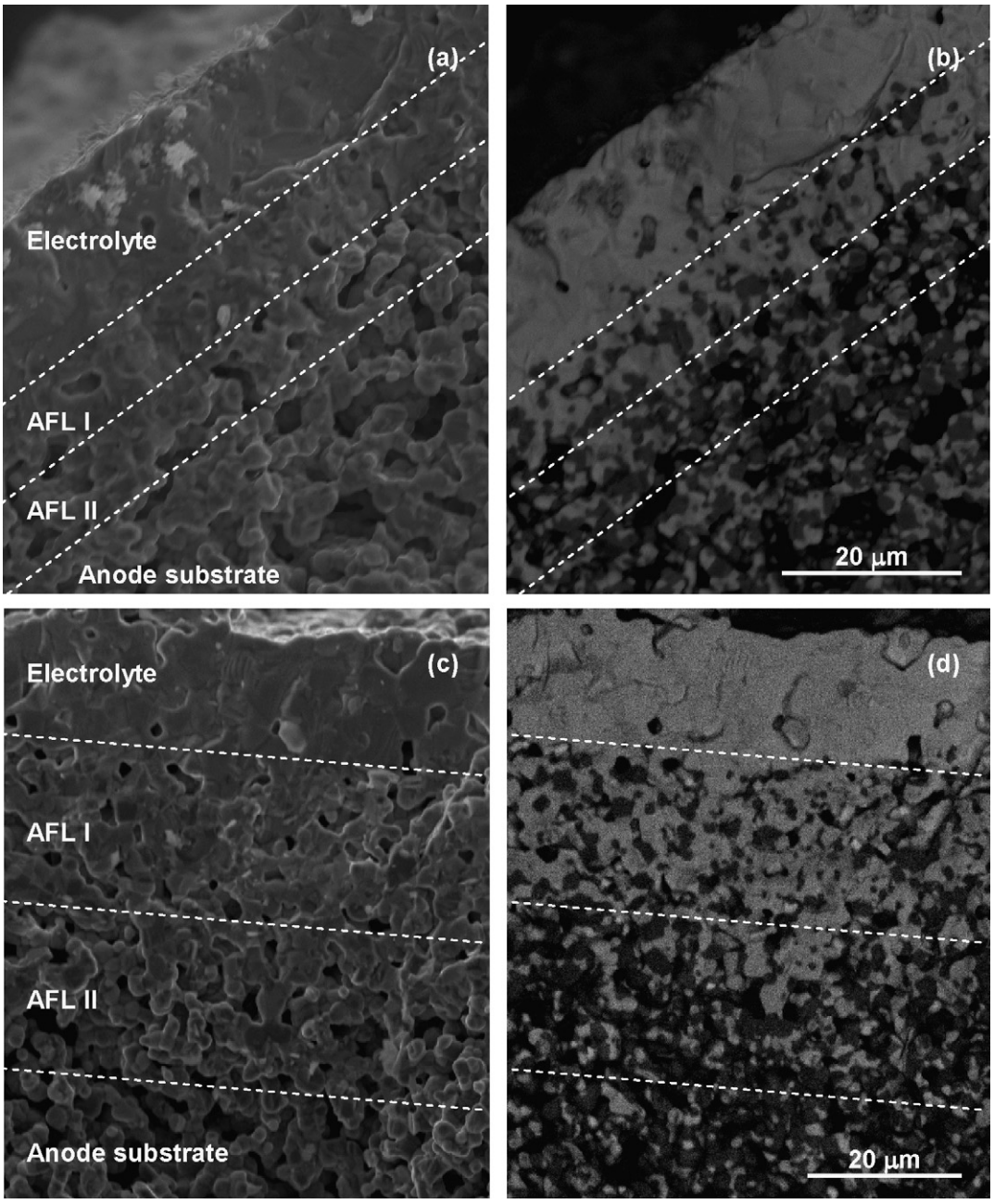

Fig. 5. SEM micrographs of the anode–electrolyte interfaces for two micro-tubular half-cells with total AFL thickness of: (a and b) 20 μm; (c and d) 40 μm.

The effect of sintering temperature on shrinkage and porosity of tubular anodes is shown in Fig. 6. The experiment carried out at 1300 °C revealed that the anode-support shrinkage was 42%, which was equivalent to the shrinkage difference between the substrate and SDC pellet during sintering at 1450 °C. However, the presence of cracks in the electrolyte film and the absence of uniformity indicated that it was necessary to slightly increase slightly the pre-sintering temperature (Fig. 7). It was found that a continuous, uniform and dense layer of electrolyte was obtained at a pre-sintering temperature of 1315 °C. Thus a good adhesion and total absence of structural defects, such as cracks or delamination in the anode–electrolyte interface were also observed. For a pre-sintering temperature of 1325 °C, the electrolyte was slightly cracked during co-sintering, due to that the shrinkage of substrate was lower than that of electrolyte, which probably generated tensile stresses on the SDC layer.

Dong et al. [25] and Bao et al. [40] reported that the shrinkages of sintered NiO–YSZ and YSZ at 1400 °C for 5 h were 21.6%, for anode made by gel-casting with a solid loading of 45%, and 20.5%, respectively. Therefore, the shrinkage of our tubular anodes was much higher than that of those fabricated by other authors. It can be attributed to that we used nanometric NiO–SDC powders (20–30 nm), agarose as a

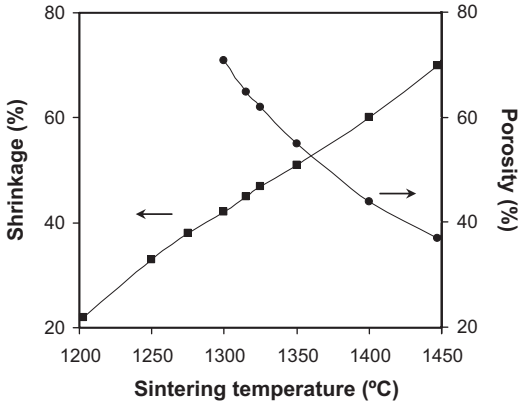

Fig. 6. Shrinkage and porosity of the NiO–SDC anode tubes as a function of the sintering temperature.

gelling agent and a low solid loading (30%) for gel-casting process, which allow to obtain homogeneous green bodies with low density before co-sintering. While the substrate shrinkage was strongly increased as the sintering temperature approached 1450 °C, the substrate porosity significantly decreased as one (Fig. 7). Despite this fact, a relatively high porosity was obtained after co-sintering (37% at 1450 °C). In addition, the porosity can be increased by reducing the NiO to Ni when the MT-SOFC is tested under hydrogen atmosphere.

3.5. Microstructure of MT-SOFCs

Fig. 8a shows the cross-sectional microstructure of an anode-supported MT-SOFC with ∼2.5 mm of outer diameter, ∼4 cm length with an active cathode length of 1.5 cm, which resulted in an active area of 1.2 cm^2. The thicknesses of anode substrate, AFL I and II, electrolyte and cathode were around 370 μm, 10 and 10 μm, 15 μm, and 40 μm, respectively. As can be seen in Figs. 8b and c, the interfaces between the electrolyte and the electrodes are very coherent, which present no observable delamination or crack. In addition, the electrolyte layer is very dense without any cracks or other visible defects. After co-sintering process, the anode substrate has a homogeneous and high porosity (37%), which will be increased when reducing the NiO to Ni under hydrogen operating condition (Fig. 8d). Anode microstructure has a uniform distribution of Ni and SDC grains, without cracks. Figs. 8e and f show the spongy microstructure of the cathode layer. After sintering, the LSC–SDC layer has a good adhesion with the dense electrolyte and low level of agglomeration with high interconnected porosity. However, the neck formation between adjacent particles was slightly occurred. There was evidence that small particles of LSC and GDC coalesced to form slightly larger aggregates. It was attributed to the use of a LSC–SDC composite layer as a cathode, in which the SDC avoided a strong coarsening of LSC particles.

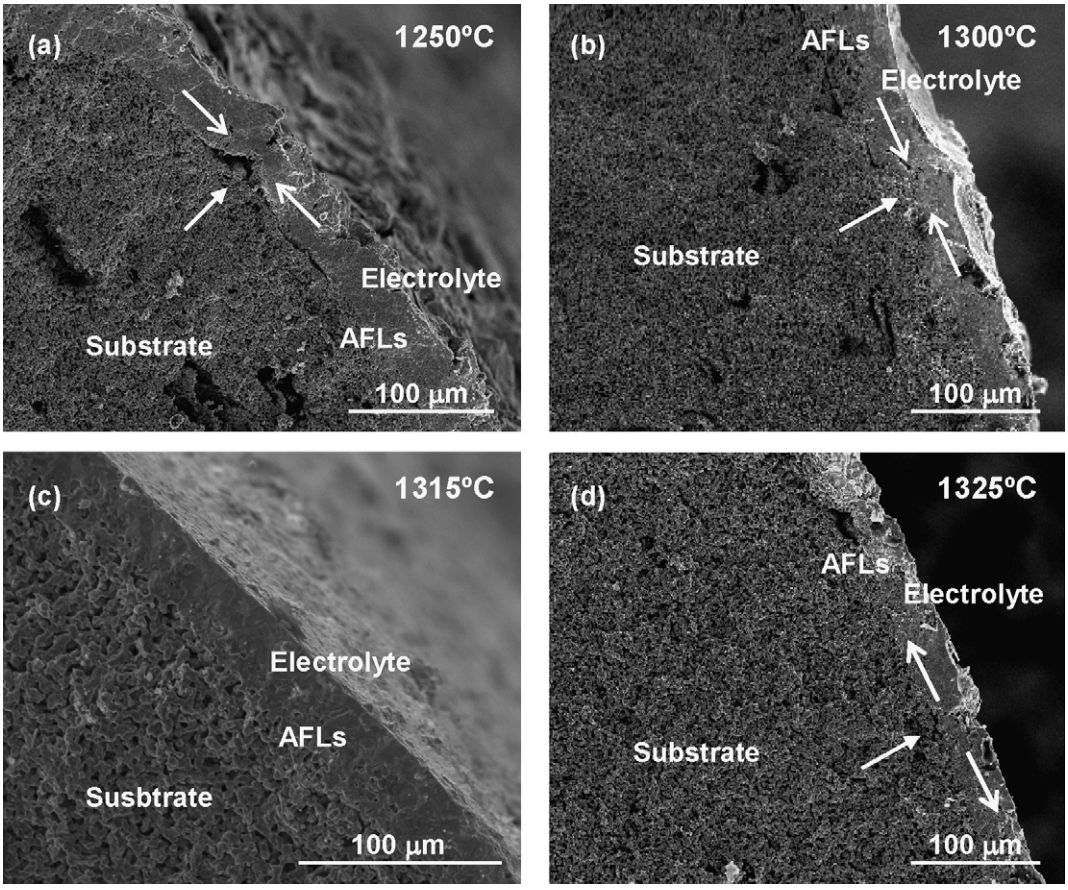

Fig. 7. SEM micrographs of anode–electrolyte interfaces for different micro-tubular half-cells after pre-sintering in air at a temperature of: (a) 1250 °C, (b) 1300 °C, (c) 1315 °C, and (d) 1325 °C; and co-sintering in air at 1450 °C.

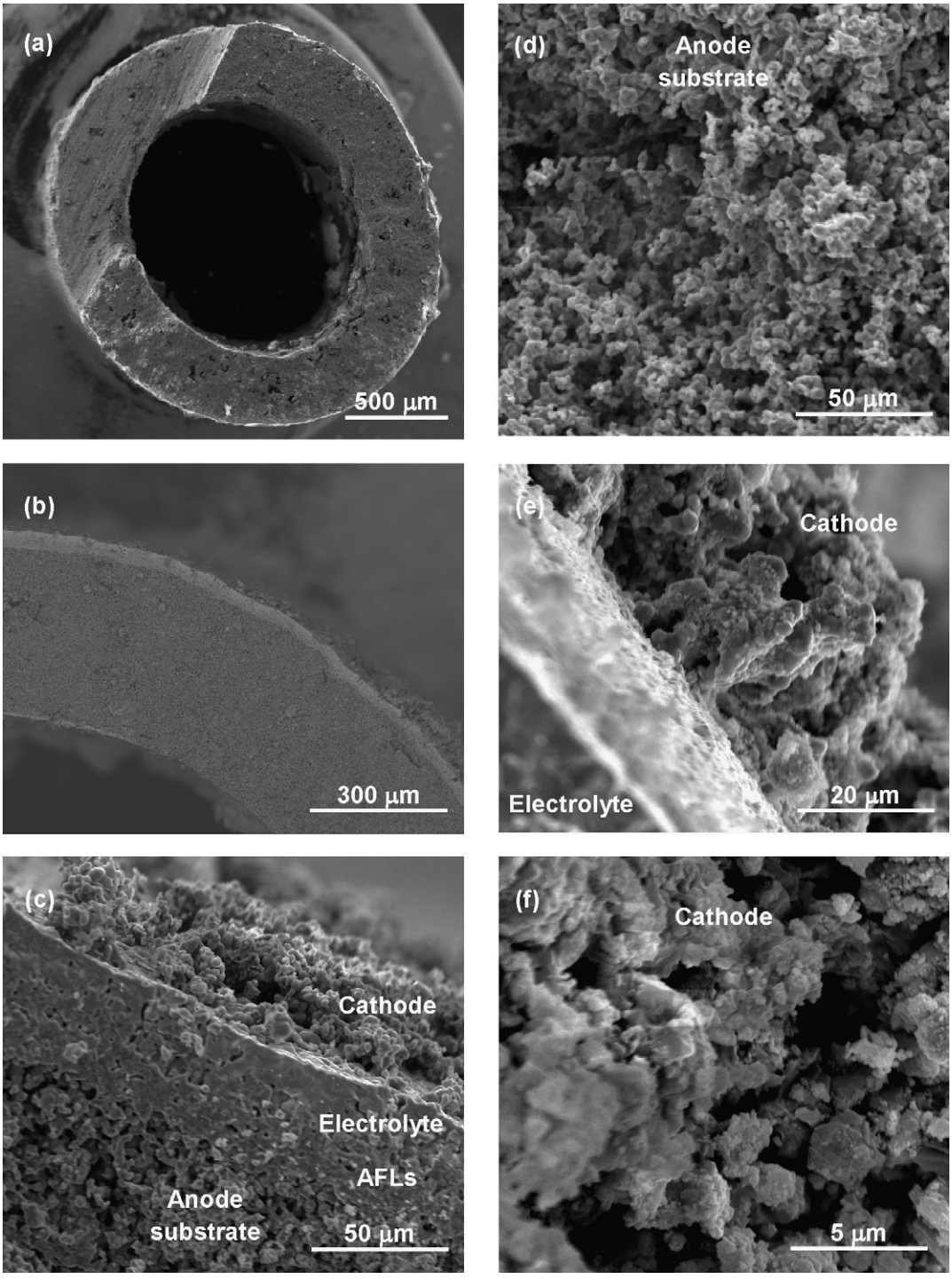

Fig. 8. SEM micrographs of cross-sectional microstructure of: (a and b) anode-supported MT-SOFC, (c) anode–electrolyte and electrolyte–cathode interfaces, (d) anode substrate, (e) cathode–electrolyte interface, and (f) cathode.

4. Conclusions

Anode-supported MT-SOFCs based on samaria-doped ceria electrolyte have been successfully obtained using gel-casting and spray-coating techniques. A suitable slurry formulation, consisting of 30 wt% powder/water and 1 wt% agarose/water, for gel-casting was prepared. This formulation was workable and useful to obtain green micro-tubular anode substrates with suitable mechanical properties, thus avoiding their plastic deformation during handling. Micro-tubular anodes were successfully shaped by a gel-casting method based on a new and simple forming technique, which operates as a syringe. Anode substrates with AFLs were pre-sintered at 1315 °C to avoid the delamination of the anode–electrolyte interface and

obtain a dense electrolyte without cracks, after co-sintering at 1450 °C for 5 h. Despite the high shrinkage of substrate (∼70%), a high anode porosity around 37% (before reducing the NiO to Ni) was obtained. On the other hand, the thickness of the AFLs and electrolyte was linearly increased with the spray-coating cycles within the range of 1–6 cycles. So, the thicknesses of anode substrate, AFL I and II, electrolyte and cathode were around 370 μm, 10 and 10 μm, 15 μm, and 20 μm, respectively. The final anode-supported MT-SOFCs presented around 2.5 mm of outer diameter. Furthermore, the use of AFLs with compositions of 30:70 and 50:50 wt% NiO–SDC allowed to obtain a continuous gradation of composition and porosity in the anode–electrolyte interface. Both interfaces between the electrolyte and the electrodes presented a good adhesion. In addition, the electrolyte layer was very dense without any cracks and pinholes. This study reveals that both gel-casting and spray-coating are industrially viable, because they are highly controllable and reproducible, and present a low cost. The real cost of the process has not widely studied. Only comparing the cost of the reagents and equipment gives an idea of the savings.

Acknowledgements

This work has been partially supported by the Ministerio de Educación y Ciencia under project MAT2008-06785-C02-01, MAT2011-23623 and the Xarxa de Referència en Materials Avançats per l'Energia (XaRMAE, Generalitat de Catalunya). The authors thank Zschimmer & Schwarz España, S.A and Laboratorios Conda for their materials supply. Experimental contributions in the preparation of this work, made by Mr. S. Fernández Quiroga and Mr. J. Ayma Padros, are gratefully acknowledged.

References

[1] EG&G Technical Services, Inc., Fuel Cell Handbook, 7th ed., University Press of the Pacific, 2004.
[2] P. Aguiar, D.J.L. Brett, N.P. Brandon, Feasibility study and techno-economic analysis of an SOFC/battery hybrid system for vehicle applications, J. Power Sources 171 (2007) 186–197.
[3] K. Kendall, M. Palin, A small solid oxide fuel cell demonstrator for microelectronic applications, J. Power Sources 71 (1998) 268–270.
[4] D. Perednis, L.J. Gauckler, Solid oxide fuel cells with electrolytes prepared via spray pyrolysis, Solid State Ionics 166 (2004) 229–239.
[5] X.Y. Zhou, A. Pramuanjaroenkij, S. Kakaç, A review on miniaturization of solid oxide fuel cell power sources. II. From system to material, NATO Sci. Peace Security Ser. C: Environ. Security (2008) 319–334.
[6] K. Yashiro, N. Yamada, T. Kawada, J. Hong, A. Kaimai, Y. Nigara, J. Mizuski, Demonstration and stack concept of quick start-up/shut-down SOFC (qSOFC), Electrochemistry 70 (12) (2002) 958–960.
[7] C.E. Hatchwell, N.M. Sammes, K. Kendall, Cathode current-collectors for a novel tubular SOFC design, J. Power Sources 70 (1998) 85.
[8] Y. Funahashi, T. Shimamori, T. Suzuki, Y. Fujishiro, M. Awano, Fabrication and characterization of components for cube shaped micro tubular SOFC bundle, J. Power Sources 163 (2) (2007) 731–736.
[9] T. Suzuki, T. Yamaguchi, Y. Fujishiro, Improvement of SOFC performance using a microtubular, anode supported SOFC, J. Electrochem. Soc. 153 (5) (2006) A925–A928.
[10] A. Boudghene Stambouli, E. Traversa, Renew. Sustainable Energy Rev. 6 (2002) 433.
[11] M. Morales, J.J. Roa, X.G. Capdevila, M. Segarra, S. Piñol, Anode-supported SOFC operated under single-chamber conditions at intermediate temperatures, Fuel Cells 11 (1) (2011) 108–115.
[12] Z. Shao, C. Kwak, S.M. Haile, Anode-supported thin-film fuel cells operated in a single chamber configuration 2T-I-12, Solid State Ionics 175 (2004) 39–46.
[13] V. Gil, J. Gurauskis, R. Campana, R.I. Merino, A. Larrea, V.M. Orera, Anode-supported microtubular cells fabricated with gadolinia-doped ceria nanopowders, J. Power Sources 196 (2011) 1184–1190.
[14] M.A. Laguna-Bercero, R. Campana, A. Larrea, J.A. Kilner, V.M. Orera, Performance and aging of microtubular YSZ-based solid oxide regenerative fuel cells, Fuel Cells 11 (1) (2011) 116–123.
[15] V.V. Kharton, F.M.B. Marques, A. Atkinson, Transport properties of solid oxide electrolyte ceramics: a brief review, Solid State Ionics 174 (2004) 135–149.
[16] M. Morales, J.J. Roa, X.G. Capdevila, M. Segarra, S. Piñol, Mechanical properties at the nanometer scale of GDC and YSZ used as electrolytes for solid oxide fuel cells, Acta Mater. 58 (7) (2010) 2504–2509.
[17] J. Fergus, R. Hui, X. Li, D.P. Wilkinson, J. Zhang, Solid Oxide Fuel Cells: Materials Properties and Performance, CRC, 2008.
[18] T. Suzuki, T. Yamaguchi, Y. Fujishiro, M. Awano, Fabrication and characterization of micro tubular SOFCs for operation in the intermediate temperature, J. Power Sources 160 (2006) 73–77.
[19] T. Suzuki, Y. Funahashi, Z. Hasan, T. Yamaguchi, Y. Fujishiro, M. Awano, Fabrication of needle-type micro SOFCs for micro-power devices, Electrochem. Commun. 10 (10) (2008) 1563–1566.
[20] C. Chen, M. Liu, L. Yang, M. Liu, Anode-supported micro-tubular SOFCs fabricated by a phase-inversion and dip-coating process, Int. J. Hydrogen Energy 36 (2011) 5604–5610.
[21] C. Fu, S.H. Chan, Q. Liu, X. Ge, G. Pasciak, Fabrication and evaluation of Ni–GDC composite anode prepared by aqueous-based tape casting method for low-temperature solid oxide fuel cell, Int. J. Hydrogen Energy 35 (2010) 301–307.
[22] J. Yang, J. Yu, Y. Huang, Recent developments in gelcasting of ceramics, J. Eur. Ceram. Soc. 31 (14) (2011) 2569–2591.
[23] A.J. Millán, I. Santacruz, A.J. Sánchez-Herencia, M.I. Nieto, R. Moreno, Gel-extrusion continuous forming technique, Adv. Eng. Mater. 4 (12) (2002) 913–915.
[24] O.O. Omatete, M.A. Janney, S.D. Nunn, Gelcasting: from laboratory development toward industrial production, J. Eur. Ceram. Soc. 17 (1997) 407–413.
[25] D. Dong, J. Gao, X. Liu, G. Meng, Fabrication of tubular NiO/YSZ anode-support of solid oxide fuel cell by gelcasting, J. Power Sources 165 (2007) 217–223.
[26] O.O. Omatete, M.A. Janney, S.D. Nunn, Gelcasting, From laboratory development toward industrial production, J. Eur. Ceram. Soc. 17 (1997) 407–413.
[27] M.A. Janney, O.O. Omatete, C.A. Walls, S.D. Nunn, R.J. Ogle, G. Westmoreland, Development of low-toxicity gelcasting systems, J. Am. Ceram. Soc. 81 (3) (1998) 581–591.
[28] J. Kong, K. Sun, D. Zhou, N. Zhang, J. Mu, J. Qiao, Ni–YSZ gradient anodes for anode-supported SOFCs, J. Power Sources 166 (2007) 337–342.
[29] A.C. Müller, D. Herbstritt, E. Ivers-Tiffée, Development of a multilayer anode for solid oxide fuel cells, Solid State Ionics 152 (2002) 537–542.
[30] W.S. Xia, H.O. Zhang, G.L. Wang, Y.Z. Yang, Functionally graded layers prepared by atmospheric plasma spraying for solid oxide fuel cells, Adv. Eng. Mater. 11 (2009) 1–2.
[31] M. Chen, B. Hee Kima, Q. Xub, B.G. Ahna, D.P. Huang, Fabrication and performance of anode-supported solid oxide fuel cells via slurry spin coating, J. Membr. Sci. 360 (2010) 461–468.
[32] C. Chen, M. Liu, L. Yang, M. Liu, Anode-supported micro-tubular SOFCs fabricated by a phase-inversion and dip-coating process, Int. J. Hydrogen Energy 36 (9) (2011) 5604–5610.
[33] D. Rotureau, D. Rotureau, J.P. Viricelle, C. Pijolat, N. Caillol, M. Pijolat, Development of a planar SOFC device using screen-printing technology, J. Eur. Ceram. Soc. 25 (12) (2005) 2633–2636.

[34] R. Yana, D. Dinga, B. Lina, M. Liua, G. Menga, X. Liu, Thin yttria-stabilized zirconia electrolyte and transition layers fabricated by particle suspension spray, J. Power Sources 164 (2) (2007) 567–571.
[35] F. Calise, G. Restuccciaa, N. Sammes, Experimental analysis of micro-tubular solid oxide fuel cell fed by hydrogen, J. Power Sources 195 (2010) 1163–1170.
[36] A. Douy, Polyacrylamide gel: an efficient tool for easy synthesis of multicomponent oxide precursors of ceramics and glasses, Int. J. Inorg. Mater. 3 (7) (2001) 699–707.
[37] S. Piñol, M. Morales, F. Espiell, Low temperature anode-supported solid oxide fuel cells based on gadolinium doped ceria electrolytes, J. Power Sources 169 (2007) 2–8.
[38] M. Morales, S. Piñol, M. Segarra, Intermediate temperature single-chamber methane fed SOFC based on Gd doped ceria electrolyte and $La_{0.5}Sr_{0.5}CoO_{3-\delta}$ as cathode, J. Power Sources 194 (2009) 961–966.
[39] E. Adolfsson, Gelcasting of zirconia using agarose, J. Am. Ceram. Soc. 89 (6) (2006) 1897–1902.
[40] W. Bao, Q. Chang, G. Meng, J. Membr. Sci. 259 (2005) 103–109.